



# Axial strength of gusset plates in buckling restrained braced frames under bidirectional monotonic loads

*S.Y. Vazquez-Colunga, C.-L. Lee & G.A. MacRae*

University of Canterbury, Christchurch.

## ABSTRACT

The commonly used design methods for gusset plates (GPs) in buckling restrained braced frames (BRBFs) only account for axial forces due to the in-plane displacement of the frame. However, real structural systems can be subjected to bidirectional loads due to earthquakes. This study aims to identify the effects of bidirectional loads on the axial strength of GPs in BRBFs by means of numerical analyses. For increasing levels of monotonic out-of-plane displacements, monotonic in-plane loading was applied to the frame by varying the axial strength of GPs due to a change in thickness, connection length and use of edge stiffeners. It was found that the axial strength of GPs is reduced as the out-of-plane displacements increase. Neglecting the effect of bidirectional loads could lead to non-conservative designs of GPs and prevent buckling restrained braces to reach their expected axial strength.

## 1 INTRODUCTION

Buckling Restrained Braces (BRBs) are now commonly used in structural systems designed to resist earthquakes. These braces are expected to dissipate energy by means of yielding under both tension and compression loads. To connect BRBs to frame elements, GPs are used. They are expected to be strong enough to allow BRBs to reach their capacity.

A common approach to design GPs under compression loads is to assume that GPs act as equivalent column elements (Thornton, 1984). The buckling load is obtained using Euler's buckling formula (Eq. 1) without considering residual stress, out-of-straightness, or boundary condition effects. This equivalent column is defined using the Whitmore width concept (Whitmore, 1952) as  $b_w$ . The length used,  $L_e$ , is usually the average of the lengths  $L_1$ ,  $L_2$  and  $L_3$  shown in Figure 1 (Vazquez-Colunga et al., 2018),

$$P_{cr} = \frac{\pi^2 EI}{(KL)^2} \quad (1)$$

Where  $P_{cr}$  is the buckling load,  $E$  the Young's modulus,  $I$  the moment of inertia, and  $K$  the effective length factor.

Modifications have been made to this method to account for additional strength due to load distribution (Yam et al., 2002). To match the buckling capacity observed in experimental tests of BRBFs, Tsai & Hsiao (2008) proposed to use an effective length factor of  $K=2.0$  to account for sway buckling. The AISC method

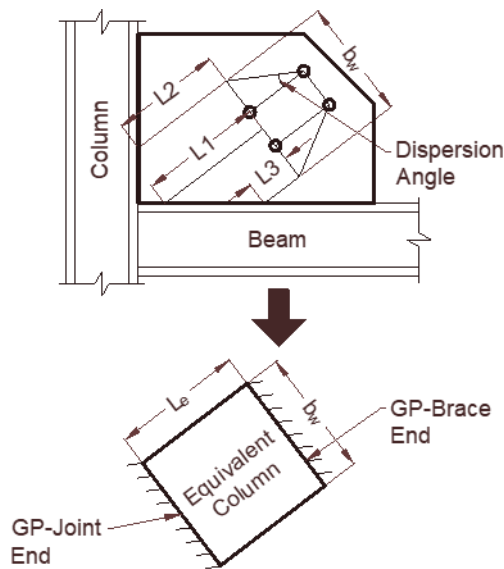


Figure 1: Whitmore width and equivalent column (Vazquez-Colunga et al., 2018).

(AISC, 2010) is also based on the equivalent column concept and includes the effects of residual stresses, eccentric loading and inelastic buckling. This method recommends an effective length factor of  $K=1.2$  for GPs with free edges and  $K=0.65$  for those with edge stiffeners. Takeuchi et al. (2016) proposed a method to check for the stability of the BRBF system, assuming out-of-plane failure mechanisms and including the effects of out-of-plane displacements, eccentric loading, initial imperfections, GP rotational stiffness, BRB end moment transfer capacity and BRB buckling capacity. Fang et al. (2015) proposed to account for the post-buckling axial strength of GPs in compression using the plate buckling equation to account for the plate action of GPs. However, most current design approaches account for the action of in-plane actions only, while in reality earthquakes will impose deformations in not only one direction.

If GPs are not properly designed, early failure at the connections may result and prevent BRBs, and the structural system, to perform as expected. Therefore, GPs must be designed considering all possible failure modes and forces acting on both in-plane and out-of-plane directions of the BRBF plane.

This study aims to quantify the performance of a number of different GPs configurations under bidirectional loading using numerical analysis of a portal frame with a single diagonal BRB. In particular, answers are sought to the following questions:

1. How do common GP design method strengths compare with numerical analysis results?
2. What is the effect of bidirectional loading on GP axial strength?
3. How can bidirectional loading be included in common design methods?
4. What is an effective alternative for increasing GP axial strength under bidirectional loading?

## 2 MODEL CALIBRATION

### 2.1 Test Description

A numerical model was validated using the results reported by Chou et al. (2012) where a BRBF was tested and GP buckling was observed. The frame width and height were 5000 mm and 3960 mm respectively. The BRB casing was made of two ASTM A36 steel channels with  $f_y = 250$  MPa and  $f_u = 400-500$  MPa. The channels were connected by A490 bolts along the brace length and was filled with concrete with a strength of 35 MPa. The core size was 112 mm x 14 mm made of steel A572 Gr. 50 with  $f_y = 345$  MPa and  $f_u = 450$  MPa. The same steel of the BRB core was used for the GPs. The top GP size was 557 x 400 mm and the

bottom was 400 x 497 mm, the thickness for both was 14 mm. Both GPs were bolted to the BRB end using 14 mm splice plates and welded to the frame elements. The frame properties can be seen in Figure 2.

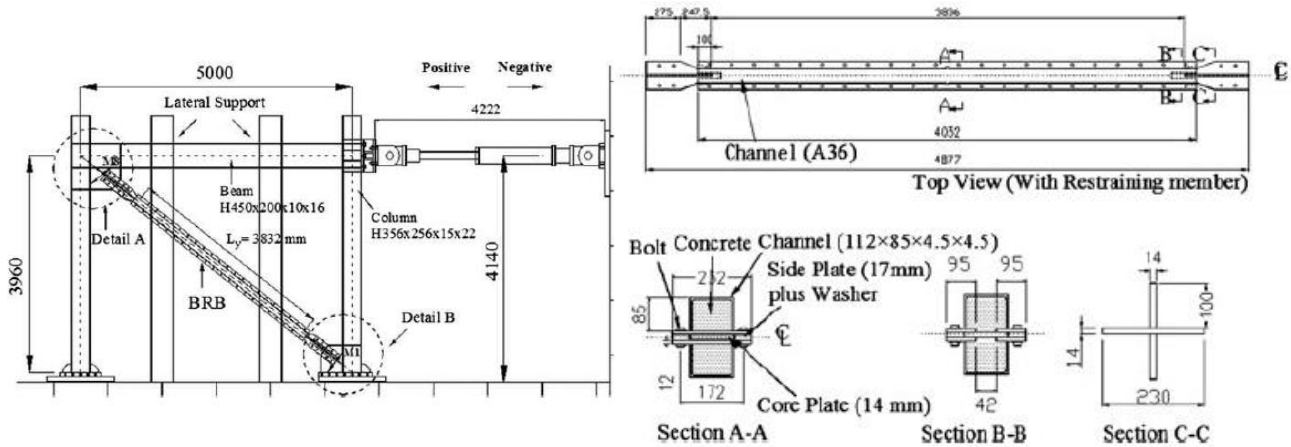


Figure 2: Frame and BRB geometry (Chou et al, 2012).

## 2.2 Modelling Techniques

For the numerical analysis, similar modelling assumptions were followed as those reported by Chou & Liu (2012). The analyses were carried out using the finite element software Abaqus 2017 (Dassault Systemes, 2016). Shell elements were used for the plates, columns, beams and the BRB connection zone. The core and casing were modelled using line elements coupled on all DOFs except the one corresponding to the BRB axial displacement. The GP-to-BRB connection was modelled by coupling together the nodes of the GPs, splice plates and BRB ends at the location of the bolts. The material was defined using the properties reported by Chou & Liu (2012) with a bilinear stress-strain relationship with kinematic hardening. The first buckling mode shape was used as the initial imperfection (out-of-straightness) for the subsequent non-linear analysis by applying a scale factor of 1/1000 times the core length. The effect of residual stresses was not included in the numerical models.

## 2.3 Comparison of Model and Test Results

During the test, the top GP buckled when the compression force in the BRB was 693 kN. From the numerical model, the buckling load obtained was 609 kN (see Figure 3). This difference of 14% might be due to the impossibility of the numerical model to account for the additional strength of the BRB under compression loads. For the test, the over strength factor was found to be equal to 1.15 as reported by Chou et al. In the numerical model, the BRB core yielded at an axial force of 591 kN while the test BRB yield load was 612 kN, this is a difference of 4%. With an acceptable discrepancy it was, therefore, assumed that this model could be used for the parametric study.

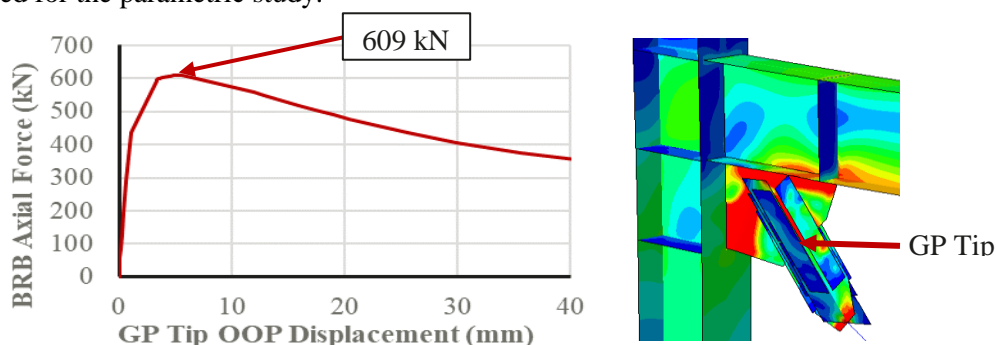


Figure 3: Gusset plate buckling load and deformations obtained from numerical model.

### 3 CASE STUDIES

To identify the effects of out-of-plane displacements on the axial strength of GPs, a parametric study with a typical range of GP parameters was carried out using finite element models of a frame with a single diagonal BRB. The parameters selected are:

1. The presence (or not) of edge stiffeners
2. Connection length
3. GP thickness

#### 3.1 Models

The frame used was the same than the used for calibration, only the GPs were modified. Two main types of GPs were selected: GPs with free edges (F) and with edge stiffeners (S). For the case of GPs with free edges, three connection lengths were studied: *LC1* (155mm), *LC2* (210mm) and *LC3* (265 mm). For the GPs with edge stiffeners, the connection lengths *LC1* and *LC2* were used. For all cases, four different thicknesses were selected: 10, 14, 18 and 22 mm. For the stiffener, its thickness was the same as the thickness of the GP analysed and its width was equal to the beam or column flange width, depending on which element was connected to the stiffener.

*Table 1: Cases Analysed for GPs with free edges.*

GP type	Connection Length Type	Thickness (mm)
F	LC1	10
		14
		18
		22
	LC2	10
		14
		18
		22
	LC3	10
		14
		18
		22

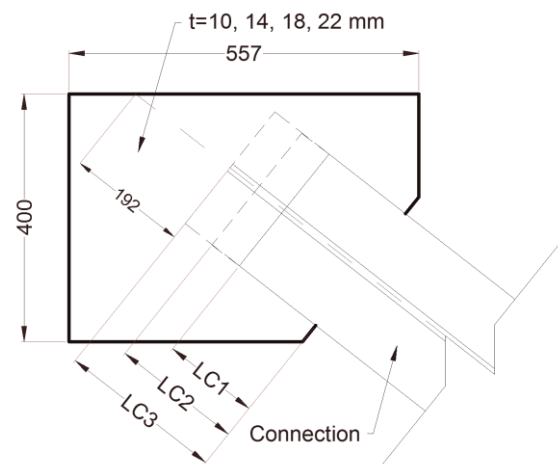
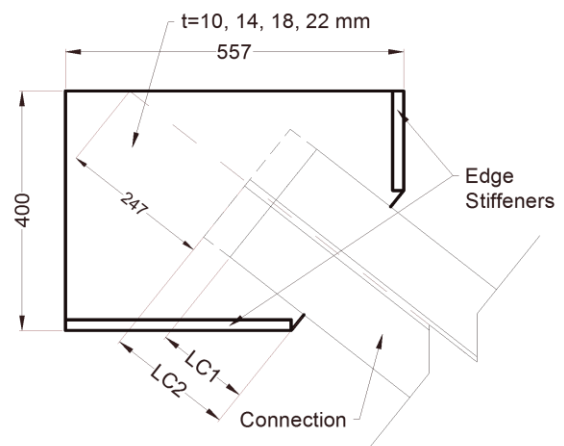


*Table 2: Cases Analysed for GPs with edge stiffeners.*

GP type	Connection Length Type	Thickness (mm)
S	LC1	10
		14
		18
		22
	LC2	10
		22



### 3.2 Displacement Application Method

The buckling load of each case was obtained by applying in-plane displacements only. This buckling load was named as the in-plane buckling load ( $P_i$ ). Five different target levels of frame out-of-plane drifts were defined as 1%, 2%, 3% 4% and 5%. For each one of the cases analysed, monotonic loading was applied following the steps shown below:

1. Apply out-of-plane displacements to the frame until the target out-of-plane drift is reached.
2. Apply in-plane displacements to the frame until GP buckling is observed.
3. Read maximum axial force at BRB core. This force is the GP reduced axial strength ( $P_r$ ).
4. Repeat Steps 1 through 3 for the next target out-of-plane drift.
5. Obtain the reduced to in-plane GP axial strength ratio ( $P_r/P_i$ ) at different drift levels for all cases.

### 3.3 Validated Model Results

The previously described methodology was applied to the validated model and the reduced axial strength was obtained when different levels of out-of-plane drifts were imposed. In addition, the  $P_r/P_o$  ratios were obtained.

It can be seen in Figure 4 that the maximum axial force of the BRB decreased as the out-of-plane drift increased. In addition, it can be noted that the GP tend to have the same strength irrespective of the imposed out-of-plane drift, at large displacements.

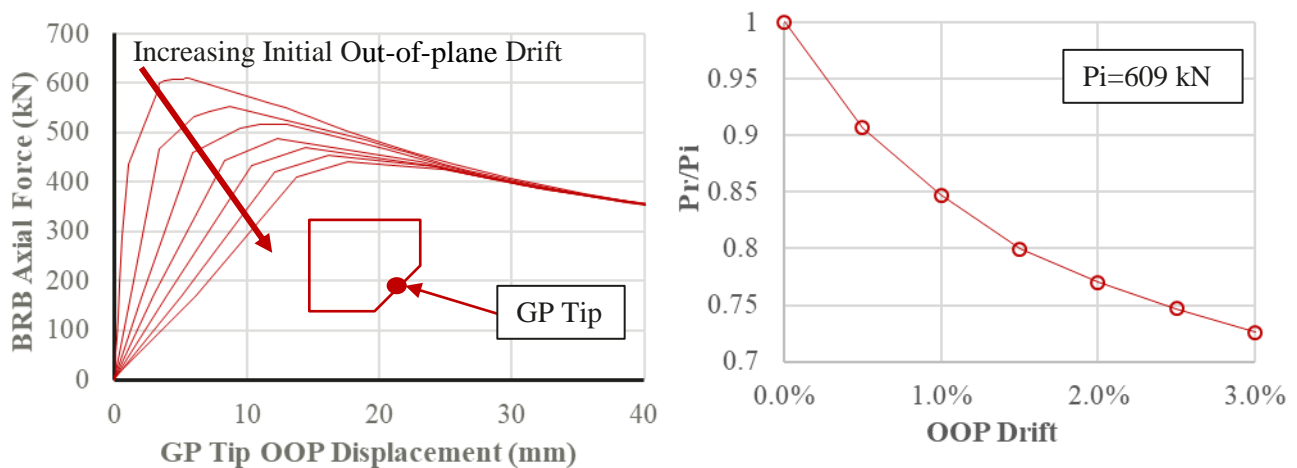


Figure 4: Reduction on axial strength for different levels of out-of-plane drifts for the calibrated model.

### 3.4 Parametric Study Results

For the cases analysed, the in-plane buckling load ( $P_i$ ) was compared with that obtained using the AISC Specification method ( $P_d$ ). To obtain the AISC buckling load, an effective length factor of  $K=2.0$  was used for the cases of GPs with free edges as proposed by Tsai & Hsiao (2008). For the cases of GPs with edge stiffeners,  $K=0.65$  was used as recommended by the AISC method (2010). The AISC to initial buckling load ratios  $P_d/P_o$  were obtained for all cases of GPs analysed. Similar to the demand to capacity ratio, the  $P_d/P_o$  ratios of larger than 1 represent non-conservative predictions of the AISC method. The results are shown in Table 3 and 4. The name for each case can be derived from Tables 1 and 2. For example, the GP with free edges  $F$  and connection length type  $LC2$  is labelled as  $FLC2$ .

Table 3: In-plane buckling load ( $P_i$ ) and AISC buckling load ( $P_d$ ) for cases of GPs with free edges.

t (mm)	FLC1			FLC2			FLC3		
	Po	Pd	Pd/Pi	Po	Pd	Pd/Pi	Po	Pd	Pd/Pi
10	206	71	0.34	236	156	0.66	270	392	1.45
14	470	194	0.41	531	429	0.81	616	976	1.58
18	641	414	0.65	905	883	0.98	937	1601	1.71
22	1202	749	0.62	1155	1388	1.20	1296	2214	1.71

\*Shaded cells belong to cases with  $P_d > P_o$

Table 4: In-plane buckling load ( $P_i$ ) and AISC buckling load ( $P_d$ ) for cases of GPs with edge stiffeners.

t (mm)	SLC1			SLC2		
	Po	Pd	Pd/Pi	Po	Po	Pd/Pi
10	421	517	1.23	527	809	1.54
14	709	898	1.27	1077	1286	1.19
18	1303	1262	0.97	1616	1743	1.08
22	1769	1613	0.91	2031	2188	1.08

\*Shaded cells belong to cases with  $P_d > P_o$

Out of 20 cases analysed of GPs under in-plane loads only, 11 of them were found to be non-conservative. The  $P_d/P_i$  ratios ranged from 0.34 to 1.58, showing that the AISC method doesn't seem to provide a predicted axial strength with a consistent accuracy. For the GPs with free edges, all cases with a LC3 connection length and the thickest case with LC2 were found to be non-conservative. This is 5 out of 12 cases. For the case of GPs with edge stiffeners, 6 out of 8 cases were found to be non-conservative. This indicates that the recommended effective length factor of 0.65 by the AISC Specification might lead to non-conservative designs when GPs with edge stiffeners are designed.

For the previous 20 cases, five different levels of out-of-plane drifts were imposed following the methodology previously described and the reduced GPs axial strength was obtained, giving a total of 120 analyses. The  $P_r/P_i$  ratio for each case and different out-of-plane drifts (OOP Drift) is shown below in Tables 5 through 9.

Table 5: Gusset plates with free edges and connection length LC1

OOP Drift	FLC1T10 Pr/Pi	FLC1T14 Pr/Pi	FLC1T18 Pr/Pi	FLC1T22 Pr/Pi
0.0%	1.00	1.00	1.00	1.00
1.0%	0.88	0.85	0.97	0.84
2.0%	0.81	0.77	0.94	0.76
3.0%	0.73	0.69	0.85	0.69
4.0%	0.69	0.64	0.80	0.64
5.0%	0.65	0.60	0.75	0.60

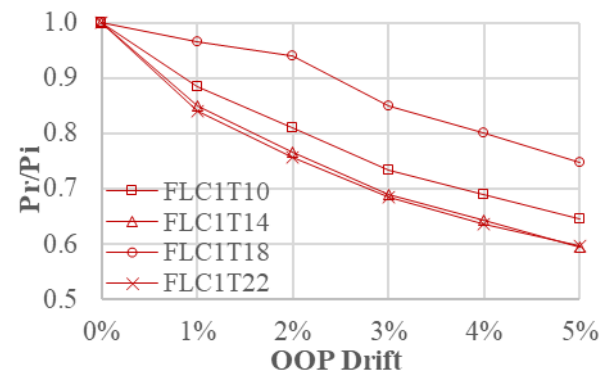


Table 6: Gusset plates with free edges and connection length LC2

OOP Drift	FLC2T10 Pr/Pi	FLC2T14 Pr/Pi	FLC2T18 Pr/Pi	FLC2T22 Pr/Pi
0.0%	1.00	1.00	1.00	1.00
1.0%	0.84	0.80	0.84	0.94
2.0%	0.73	0.74	0.68	0.70
3.0%	0.72	0.69	0.68	0.75
4.0%	0.67	0.64	0.61	0.67
5.0%	0.62	0.59	0.59	0.67

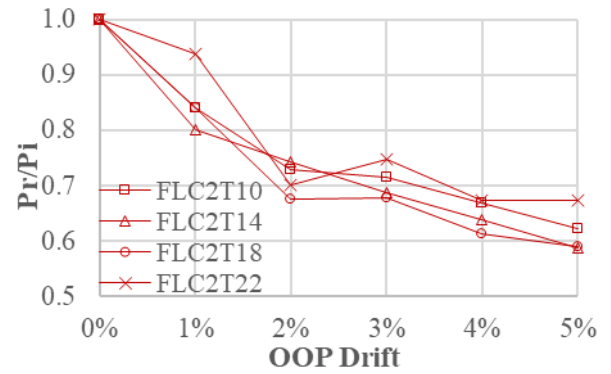


Table 7: Gusset plates with free edges and connection length LC3

OOP Drift	FLC3T10 Pr/Pi	FLC3T14 Pr/Pi	FLC3T18 Pr/Pi	FLC3T22 Pr/Pi
0.0%	1.00	1.00	1.00	1.00
1.0%	0.88	0.77	0.88	0.95
2.0%	0.80	0.72	0.81	0.85
3.0%	0.74	0.68	0.74	0.79
4.0%	0.70	0.64	0.69	0.73
5.0%	0.67	0.59	0.65	0.69

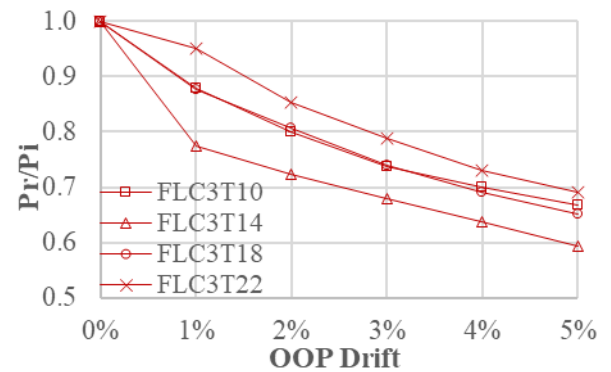


Table 8: Gusset plates with edge stiffeners and connection length LC1

OOP Drift	SLC1T10 Pr/Pi	SLC1T14 Pr/Pi	SLC1T18 Pr/Pi	SLC1T22 Pr/Pi
0.0%	1.00	1.00	1.00	1.00
1.0%	0.83	0.95	0.91	0.89
2.0%	0.78	0.92	0.81	0.78
3.0%	0.74	0.87	0.74	0.73
4.0%	0.69	0.80	0.68	0.67
5.0%	0.64	0.75	0.63	0.63

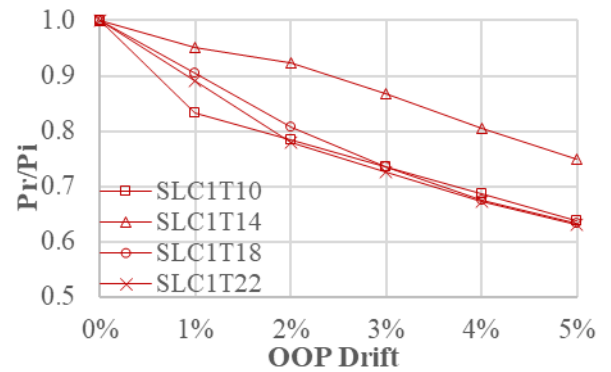
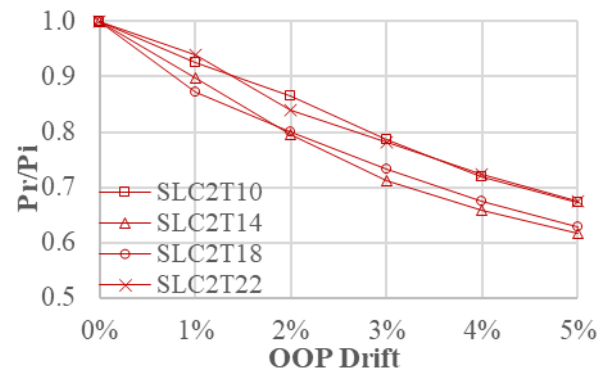


Table 9: Gusset plates with edge stiffeners and connection length LC2

OOP Drift	SLC2T10 Pr/Pi	SLC2T14 Pr/Pi	SLC2T18 Pr/Pi	SLC2T22 Pr/Pi
0.0%	1.00	1.00	1.00	1.00
1.0%	0.93	0.90	0.87	0.94
2.0%	0.87	0.80	0.80	0.84
3.0%	0.79	0.71	0.73	0.78
4.0%	0.72	0.66	0.68	0.72
5.0%	0.67	0.62	0.63	0.68



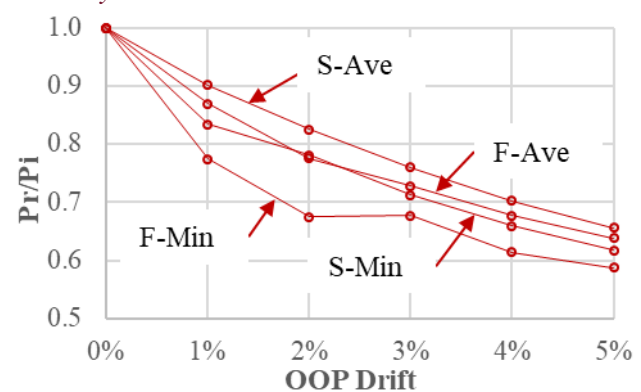
In all cases, a reduction on axial strength was observed and this reduction increased as the imposed out-of-plane drift increased. Taking an out-of-plane drift of 2% as reference, the minimum Pr/Pi ratio was found to

be 0.68 and 0.78 for the case of GPs with free edges and edge stiffeners, respectively. A summary of these results can be seen in Table 10.

Taking again a 2% out-of-plane drift as reference and using the average Pr/Pi ratios, they were found to be equal to 0.78 and 0.82 for the GPs with free edges and edge stiffeners, respectively. This means that the Pd/Pi ratios obtained using the AISC method should be  $Pd/Pi < 0.78$  and  $Pd/Pi < 0.82$  for GPs with free edges and edge stiffeners respectively, to provide a conservative design when a BRBF is designed to reach an out-of-plane drift of 2%. With this consideration, more designs became non-conservative of those presented in Table 3 and 4. In total, only 6 out of 20 design can be assumed as conservative, which means that 70% of the GPs designs could fail if the frame deforms until reaching an out-of-plane drift of 2%. If the average Pr/Pi ratios for GPs with free edges and edge stiffeners were 0.78 and 0.82 respectively, a safety factor of 0.75 (slightly smaller than both of them) appears to be reasonable for this drift level to provide a conservative design, but further study must be performed. If a 1% out-of-plane drift is used as reference and coupled with the in-plane action, the previous safety factor of 0.75 will cover all Pr/Pi ratios including the minimum ratios obtained.

Table 10: Average and minimum Pr/Pi ratios for the GPs analysed

OOP Drift	Free Edges		Edge Stiffeners	
	F-Ave	F-Min	S-Ave	S-Min
0.0%	1.00	1.00	1.00	1.00
1.0%	0.87	0.77	0.90	0.83
2.0%	0.78	0.68	0.82	0.78
3.0%	0.73	0.68	0.76	0.71
4.0%	0.68	0.61	0.70	0.66
5.0%	0.64	0.59	0.66	0.62



It can be observed from Table 10 that, at all levels of out-of-plane drifts, the reduction in axial strength was always higher for GPs with free edges than that for those with edge stiffeners. In average, the axial strength reduction of GPs with free edges was 20% higher than that of GPs with edge stiffeners. This could be due to the additional flexural stiffness provided by the edge stiffeners to the GP. Further study is continuing to fully understand this results, as well as those of members under cyclic loading.

It is important to note that the results obtained dependent on the rotational flexibility of the boundary elements. The GPs axial strength could be reduced as the rotational restraints provided by the beam and column are reduced. In addition, the effect of residual stresses needs to be included as it is likely to reduce GPs axial strength. The effects of the rotational flexibility of the boundary elements and residual stresses will be included in future studies.

### 3.5 Conclusions

Numerical analyses were performed on a BRBF with different GP configurations under monotonic loading to identify the effects of bidirectional loading on GP axial strength. It was found that:

1. The AISC method buckling loads ( $P_d$ ) obtained for 20 cases analysed ranged from 0.34 to 1.58 times those obtained by means of calibrated numerical analyses ( $P_i$ ) when only in-plane displacements were applied. For GPs with free edges, 5 out of 12 design predictions were found to be non-conservative. An effective length factor of  $K=2.0$  produced conservative designs for GPs with short connection lengths and became non-conservative for GPs with longer connection lengths. For GPs with edge stiffeners, 6

out of 8 design predictions were found to be non-conservative. These results suggest that an effective length factor greater than  $K=0.65$  should be used for this type of GPs.

2. Applying out-of-plane displacements on GPs in addition to in-plane displacements reduced their axial strengths. This reduction increased as the applied out-of-plane displacements increased. Taking an out-of-plane drift of 2% as reference, the minimum AISC to initial buckling load ratio  $P_d/P_i$  was 0.68 for GPs with free edges and 0.78 for those with edge stiffeners. The average  $P_d/P_i$  ratio at the same drift level was 0.78 for GPs with free edges and 0.82 for those with edge stiffeners. A  $P_d/P_i$  ratio equal to 0.75 will provide a conservative estimation of the reduction on axial strength for the cases studied for an out-of-plane drift level of 2%. Different levels of out-of-plane drifts coupled to in-plane actions will require different  $P_d/P_i$  ratios.
3. Following the AISC Specification method and taking a 2% out-of-plane drift as reference, only 6 out of 20 cases were found to be conservative. However, by limiting the demand to 75% of the AISC method capacity, the strength was sufficient for the cases studied.
4. For the cases analysed, the presence of stiffeners of the sizes used increased the GP strength between 1.5 to 2.2 times that of GPs with free edges. Furthermore, the axial strength reduction was on average about 20% greater for GPs with free edges than for those with edge stiffeners. It is recommended to use edge stiffeners as the first alternative to increase GPs axial performance.

The previous conclusions are applicable to GPs with a similar configuration and boundary conditions in the range than the analysed in this study and those of the test performed by Chou et al. Further study will be performed to cover a wider range of BRBFs configurations.

## 4 REFERENCES

- AISC. 2010. *Specification for Structural Steel Buildings, ANSI-AISC 360-10*, American Institute of Steel Construction, Chicago, USA.
- Chou, C.-C. & Liu, J.-H. 2012. Frame and Brace Action Forces on Steel Corner Gusset Plate Connections in Buckling-Restrained Braced Frames, *Earthquake Spectra*, Vol 28(2) 531-551.
- Chou, C.-C., Liu, J.-H. & Pham, D.-H. 2012. Steel buckling-restrained frames with single and dual corner gusset connections: seismic test and analyses, *Earthquake Engineering and Structural Dynamics*, 1137-1156.
- Dassault Systemes. 2016. *Abaqus/CAE 2017*. Dassault Systemes Simulia Corp., Rhode Island, USA.
- Fang, C., Yam, M.C.H., Zhou, X. & Zhang, Y. 2015. Post-buckling resistance of gusset plate connections: Behaviour, strength, and design considerations, *Engineering Structures*, Vol 99 9-27.
- Takeuchi, T., Matsui, R. & Mihara, S. 2016. Out-of-plane stability assessment of buckling-restrained braces including connections with chevron configuration, *Earthquake Engineering & Structural Dynamics*, Vol 45 1895-191.
- Thornton, W.A. 1984. Bracing Connections for Heavy Construction, *Engineering Journal (AISC)*, No. 3 139-148.
- Tsai, K.-C. & Hsiao, P.-C. 2008. Pseudo-dynamic test of a full-scale CFT/BRB frame—Part II: Seismic performance of buckling-restrained braces and connections, *Earthquake Engineering and Structural Dynamics*, 1099-1115.
- Vazquez-Colunga, S.Y., Lee, C.-L. & MacRae, G.A. 2018. Effects of Out-of-Plane Displacements on Load Capacity of Gusset Plates in Buckling Restrained Braced Frames, *The 9<sup>th</sup> International Conference on the Behaviour of Steel Structures in Seismic Areas, 14-17 February 2018*.
- Whitmore, R.E. 1952. *Experimental Investigation of Stresses in Gusset Plates*. University of Tennessee. Bulletin No. 16.
- Yam, M.C.H. & Cheng, J.J.R. 2002. Behavior and design of gusset plate connections in compression, *Journal of Constructional Steel Research*, Vol 58 1143-1159.